Hypertension Research (2015) 38, 821–828
© 2015 The Japanese Society of Hypertension All rights reserved 0916-9636/15
www.nature.com/hr

ORIGINAL ARTICLE

Upregulation of canonical transient receptor potential channel in the pulmonary arterial smooth muscle of a chronic thromboembolic pulmonary hypertension rat model

Xin Yun[1,2], Yuqin Chen[1], Kai Yang[1,2], Sabrina Wang[2], Wenju Lu[1] and Jian Wang[1,2]

Chronic ligation of the left main pulmonary artery (PA) results in pulmonary vascular remodeling and sustained vasoconstriction. This method has been used to generate a postobstructive pulmonary vasculopathy model to mimic severe chronic thromboembolic pulmonary hypertension (CTEPH). The aim of this study was to examine the cellular and molecular mechanisms underlying CTEPH and to provide evidence for potential treatments. The CTEPH rat model was induced by surgical left PA ligation (LPAL). Right ventricular systolic pressure (RVSP), lung histochemistry and plasma D-dimer measurements were carried out to evaluate the model. A fluorescence microscope was used to measure the basal intracellular Ca^{2+} concentration ($[Ca^{2+}]_i$) and store-operated Ca^{2+} entry (SOCE) in rat distal pulmonary arterial smooth muscle cells through a Fura-2 fluorescence-based method. The expression of the canonical transient receptor potential channel 1 (TRPC1) and TRPC6 was determined by western blotting and real-time quantitative PCR in isolated distal pulmonary arteries (PA). At the time points of 2 and 5 weeks postsurgery, the RVSP showed significant increases in the LPAL groups in comparison with the respective control groups. LPAL also led to right ventricular hypertrophy (RVH), distal pulmonary arterial remodeling in unobstructed territories and persistently higher plasma D-dimer levels. Increases of the basal $[Ca^{2+}]_i$ and SOCE in LPAL were associated with a clear upregulation of TRPC1 and TRPC6 expression in the distal PA. Our study demonstrated that LPAL successfully reproduced the vascular tone changes that mimic CTEPH pathogenesis. In this model, the increased RVSP and RVH are likely related to enhanced SOCE and upregulated TRPC1 and TRPC6 expression levels in the distal PA.
Hypertension Research (2015) **38,** 821–828; doi:10.1038/hr.2015.80; published online 9 July 2015

Keywords: chronic thromboembolic pulmonary hypertension (CTEPH); pulmonary artery ligation; SOCE; TRPC

INTRODUCTION

Chronic thromboembolic pulmonary hypertension (CTEPH) is a notoriously underdiagnosed and life-threatening disease. It is generally defined as a pulmonary arterial obstruction by one or more episodes of acute pulmonary embolism.[1] Once vascular occlusion is severe enough to cause an increase in the pulmonary vascular resistance (PVR), and subsequent elevation in pulmonary arterial pressure, pulmonary vascular remodeling and contraction would appear and progressively lead to the development of PH. In addition, up to two-thirds of the patients do not have a history of acute pulmonary embolism or the symptoms appear to be clinically silent.[2] To better understand the pathogenesis of CTEPH, especially to elucidate its molecular mechanisms, an experimental rat model has been designed to mimic PH via pulmonary artery (PA) ligation.[3–5]

Evidence from clinical studies has indicated that CTEPH patients can be cured surgically by pulmonary endarterectomy, which can effectively normalize pulmonary PVR. However, a number of CTEPH patients quickly develop persistent PH again after surgery.[6] A study by Sacks *et al.*[7] showed that CTEPH patients with low obstruction suffer from extremely high pulmonary arterial pressure, suggesting that pulmonary vascular obstruction is not the only cause for the elevated PVR. Consequently, sustained PVR elevation still exists after pulmonary endarterectomy most likely owing to the established vascular wall thickening, which is related to the excessive proliferation and migration of pulmonary arterial smooth muscle cells (PASMCs).[8,9] Based on the evidence provided above, we assume that CTEPH patients might share similar pathogenic mechanisms for the development of pulmonary vascular remodeling as PH patients.[10]

[1]Guangzhou Institute of Respiratory Diseases, State Key Laboratory of Respiratory Diseases, The First Affiliated Hospital, Guangzhou Medical University, Guangzhou, Guangdong, People's Republic of China and [2]Division of Pulmonary and Critical Care Medicine, Johns Hopkins University School of Medicine, Baltimore, MD, USA
Correspondence: Dr W Lu or Dr J Wang, Guangzhou Institute of Respiratory Diseases, State Key Laboratory of Respiratory Disease, The First Affiliated Hospital, Guangzhou Medical University, 151 Yanjiang Road, Guangzhou, Guangdong 510120, China.
E-mail: wlu92@yahoo.com or jwang31@jhmi.edu
Received 21 October 2014; revised 22 May 2015; accepted 29 May 2015; published online 9 July 2015

During the past few years, researchers have been focusing on the mechanisms underlying PH in multiple models, in which intracellular Ca^{2+} is believed to be a critical effecter. Our previous studies and those of other groups have shown that the elevation of the intracellular free Ca^{2+} concentration ($[Ca^{2+}]_i$) has a vital role in the development of pulmonary vasoconstriction and vascular remodeling during PH pathogenesis. In chronic hypoxia-induced pulmonary hypertension and monocrotaline-induced pulmonary hypertension animal models, enhanced store-operated Ca^{2+} entry (SOCE) via the store-operated Ca^{2+} channel (SOCC) largely changes the elevated $[Ca^{2+}]_i$ in PASMCs.[11–14] SOCC is known to be composed of the canonical transient receptor protein channel (TRPC) family that contains seven different members, among which TRPC1, TRPC4 and TRPC6 are predominantly expressed in rat distal PASMCs.[15] Chronic hypoxia selectively upregulates the expression of TRPC1 and TRPC6 but not TRPC4 expression in the rat distal PA and cultured PASMCs.[13]

Based on the known mechanisms from both chronic hypoxia-induced and monocrotaline-induced pulmonary hypertension and considering that CTEPH also shares physiological and pathophysiological changes similar to other PH models, we hypothesized that the TRPC–SOCE–$[Ca^{2+}]_i$ signaling axis might also have a crucial role in the pathogenesis of CTEPH. We first generated a left PA ligation (LPAL) experimental rat model to mimic CTEPH and then investigated the changes of the TRPC–SOCE–$[Ca^{2+}]_i$ signaling axis during the development of this type of PH upon the application of this CTEPH rat model. Given that the mechanisms of CTEPH are currently lacking, these results will contribute to a better understanding of the underlying mechanisms of CTEPH and suggest new therapeutic targets for CTEPH patients.

METHODS

Surgical procedure for PA ligation

All of the animal procedures were approved by the Animal Care and Use Committee of Guangzhou Medical University. Adult SPF male Sprague-Dawley rats (250–300 g, provided by Experimental Animal Center of Guangdong Province) were randomly allocated to three groups ($n=5$ in each group): (1) dissection without ligation (sham group); (2) no treatment (control group); and (3) LPAL (LPAL group). Observational studies were taken at the time points of 2 and 5 weeks after the surgery (sham and LPAL), accompanied by parallel controls. Animals were anesthetized using pentobarbital sodium (35 mg kg^{-1} intraperitoneally). After endotracheal intubation, intermittent positive-pressure ventilation was provided at a tidal volume of 8 ml kg^{-1}, with a respiratory rate at 85 cycles min^{-1}. Left lateral thoracotomy was performed at the third intercostal followed by the sectioning of the intercostal muscles to expose the left lung. The left lung was moved back so that the PA of the left lung lobe was on top of the airway. Forceps were carefully used to separate the PA from the left mainstem bronchus at the hilum of their natural borders. The PA was ligated with suture (size 6-0), and the thoracotomy was closed with a suture (size 4-0) while the animal was placed on positive end-expiratory pressure. Lidocaine (2 mg kg^{-1}) was injected at the incision site for analgesia. Animals were then disconnected from the ventilator, extubated when respiration had been stabilized and allowed to recover. Rats in the sham groups were treated similarly except for the ligation. No operating procedures were performed on the control groups.

Hemodynamic measurements and lung histochemistry

The right ventricular systolic pressure (RVSP) and right ventricular hypertrophy (RVH) were measured using the same method as we described previously.[16] Briefly, a 23-gauge needle filled with heparinized saline was connected to a pressure transducer and inserted via the diaphragm into the right ventricle. The RVSP was then recorded and measured using a 16-channel physiological instrument for small animals from BIOPAC (Goleta, CA, USA). The RVH was evaluated as the wet weight ratio of the right ventricle to the left ventricle with the septum (RV/(LV+S)). To visualize intrapulmonary vessels, lung tissue samples were taken from animals of different groups and placed in 10% formalin for 24 h, followed by hematoxylin and eosin staining performed on paraffin-embedded lung cross sections (5 μm). Histological thickening/changes were evaluated using the Image-Pro analytic software (Silver Spring, MD, USA). Similar populations of vessels in lung sections from each animal were examined. Vessel wall area (WA) and total vessel area (TA) were measured, and the average of the WA/TA ratios as well as the mean media thickness of the pulmonary arterioles were calculated and compared across different groups.

Determination of D-dimer concentration in plasma by enzyme-linked immunosorbent analysis

The concentration of rat D-dimer was determined using an ELISA Kit (Uscn Life Science, Wuhan, China), which measured the color intensity by a microplate reader, according to the manufacturer's instructions.

Distal PA isolation and PASMC culture

Rat distal PAs (>fourth generation) were isolated from the right lung lobe of anesthetized male Sprague-Dawley rats from the different treatment groups and denuded from adventitia and endothelium as we previously described.[13,15,16] PASMCs were enzymatically digested from denuded distal PAs, harvested and cultured with Smooth Muscle Growth Medium-2 (Clonetics, Allendale, NJ, USA) containing 0.5% fetal bovine serum on coverslips for 2 days and then prepared for calcium imaging experiments.

Intracellular Ca^{2+} imaging measurement

The intracellular Ca^{2+} and SOCE were measured in PASMCs using fura-2 and a Nikon TSE 100 Ellipse inverted microscope (Nikon, Melville, NY, USA) digital fluorescence imaging system as previously described. Data were collected with the InCyte software (Cincinnati, OH, USA). For the SOCE measurements, PASMCs were perfused for 10 min with Ca^{2+}-free solution to remove extracellular Ca^{2+}, containing 5 μM nifedipine, to exclude the effect of calcium entry through L-type voltage-dependent Ca^{2+} channels, and 10 μM cyclopiazonic acid (CPA), to deplete sarcoplasmic reticulum calcium stores.[13,15–17]

Real-time quantitative PCR

Total RNA was extracted using the TRIzol (Invitrogen, Grand Island, NY, USA) method for de-endothelialized distal PA. As previously described, reverse transcription was performed using a TaKaRa RT Kit (Takara, Dalian, China), with a reaction mixture 20 μl in volume containing 1000 ng of total RNA. This step was followed by real-time quantitative PCR, which was performed using Scofast EvaGreen SuperMix (Bio-Rad, Carlsbad, CA, USA) in a CFX96 real-time system (Bio-Rad). The primers were synthesized by TaKaRa Biotechnology, and the sequences are listed here. Rat TRPC1 primers: sense, 5′-AGCCTCTTGACAAACGAGGA-3′; antisense, 5′-ACCTGACATCTGTCCG AACC-3′; TRPC6 primers: sense, 5′-TACTGGTGTGCTCCTTGCAG-3′; antisense, 5′-GAGCTTGGTGCCTTCAAATC-3′; and 18S primers: sense, 5′-GCA ATTATTCCCCATGAACG-3′; antisense, 5′-GGCCTCACTAAACCATCCAA-3′. The expression levels of TRPC1 and TRPC6 were normalized to 18S, which served as an internal house-keeping control.[16]

Western blotting analysis

Rat distal de-endothelialized PA samples were sonicated in a Laemmli sample buffer that included 62.5 mM Tris-HCl (pH 6.8), 10% glycerol, 5% protease inhibitor cocktail, 2% sodium dodecyl sulfate, 1 mM EDTA and 200 μM 4-(2-aminoethyl)benzenesulfonyl fluoride hydrochloride. As previously described, protein expression was measured by immunoblotting.[13,15,16] Protein samples were resolved by 8% sodium dodecyl sulfate-polyacrylamide gel electrophoresis, and separated proteins were then transferred onto polyvinylidene difluoride membranes (pore size 0.45 μM, Bio-Rad). Membranes were blocked by 5% nonfat dry milk in Tris-buffered saline containing 0.2% Tween 20, blotted with affinity-purified rabbit polyclonal antibodies specific for TRPC1 (Santa Cruz Biotechnology, Santa Cruz, CA, USA), TRPC6 (Alomone Laboratories, Jerusalem, Israel) or mouse monoclonal antibodies to α-actin

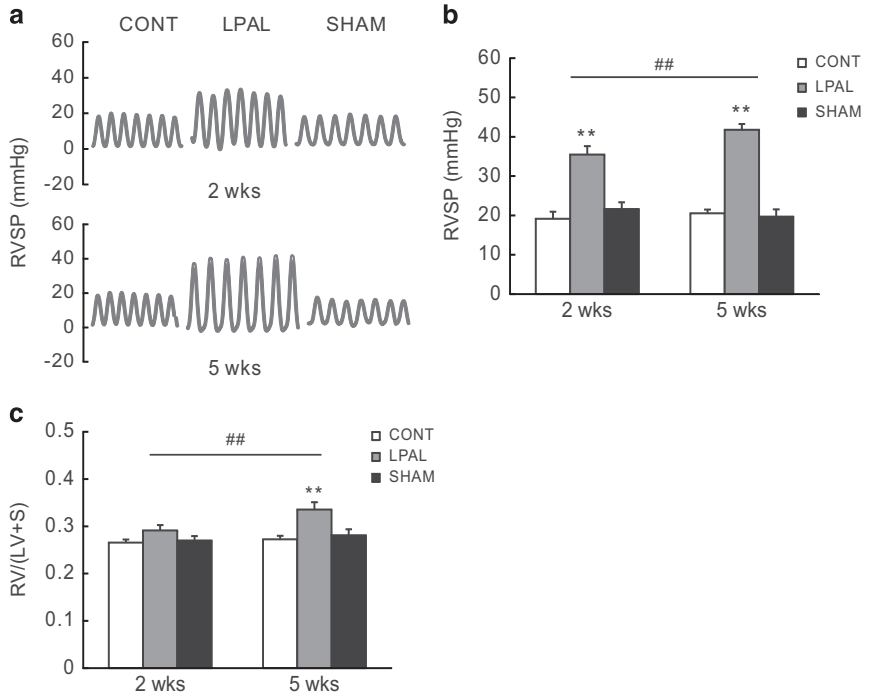

Figure 1 Effects of chronic LPAL on the rats' right ventricular systolic pressure, mean pressure and right ventricular hypertrophy (mean ± s.e.m., $n=5$). Animals were randomly allocated to one of the three groups: no treatment as the control group (CONT), left pulmonary artery ligation (LPAL), and sham surgery (SHAM). (**a**) Representative traces of RVSP of each group of animals. (**b**, **c**) Bar graphs showing the right ventricular systolic pressure (RVSP) and the index of right ventricular hypertrophy (RV/LV+S). $^{**}P<0.01$ *vs.* respective CONT and SHAM group, and $^{\#\#}P<0.01$ *vs.* 5 weeks LPAL group. A full color version of this figure is available at the *Hypertension Research* journal online.

(Sigma, St Louis, MO, USA) and then incubated with the appropriate secondary antibody. Blots were detected using an enhanced ECL HRP Chemiluminescent substrate reagent (Bio-Rad).

Statistical analysis

Data were analyzed using the SPSS (Statistical Package for the Social Sciences) 13.0 statistical software (Armonk, NY, USA). The data are represented as the mean ± s.e.m., and '*n*' is the number of experiments performed equaling the numbers of animals used to obtain PAs or PASMCs. For comparisons between groups, two-way analysis of variance with Tukey *post-hoc* test were used. *P*-values <0.05 were considered statistically significant.

RESULTS

LPAL rats exhibited a marked elevation in RVSP and RVH

All animals survived after the surgical operation. Our results showed that the RVSP was significantly ($P<0.01$) higher in the LPAL groups at both 2 and 5 weeks after surgery compared with the respective sham groups (Figures 1a and b). In detail, at the 2-week time point, the RVSP of LPAL group was 35.50 ± 2.13 mm Hg, the sham group's RSVP was 21.61 ± 1.73 mm Hg and the control group's RSVP was 19.17 ± 1.80 mm Hg. At 5 weeks, the RVSP of the LPAL group was 41.79 ± 1.46 mm Hg, the sham group's was 19.72 ± 1.83 mm Hg and the control group's was 20.55 ± 0.94 mm Hg. From 2 to 5 weeks, there was also a significant increase of RVSP in the LPAL group. However, there was no significant difference in RVSP between the sham and the control groups. For the RVH index at 2 weeks, as shown in Figure 1c, the RV/(LV+S) in the LPAL group was 0.29 ± 0.01, that of the sham group was 0.27 ± 0.01 and that of the control group was 0.27 ± 0.01. There were no significant differences among these groups. However, at 5 weeks, the RV/(LV+S) in the LPAL group was 0.34 ± 0.02, which was significantly higher than that of the sham group (0.28 ± 0.01) ($P<0.01$). The RV/(LV+S) of the control group was 0.27 ± 0.01, and there was no significant difference in the control group *vs.* the sham group. These results suggested that, after 5 weeks of surgical ligation, chronic ligation induced continuous pulmonary vascular obstruction, followed by the development of RVH.

LPAL promoted rat distal pulmonary arterial remodeling

As shown in Figure 2, the structure of the intima of the small distal PA in the rats from control and sham groups was intact and smooth, without obvious thickening of the smooth muscle medium layer. However, in the LPAL groups at 2 (Figure 2b) and 5 weeks (Figure 2e) postsurgery, the distal PA walls were obviously thickened in the smooth muscle medium wall, as examined by histochemistry.

LPAL elevated plasma D-dimer concentrations

Plasma D-dimer levels were used as an indicator of thrombosis in clinical practice. Figure 3 illustrates the measured plasma D-dimer levels from postsurgery and control rats at both the 2- and 5-week time points. In detail, at 2 weeks, the plasma D-dimer concentration was 7.82 ± 1.43 ng ml^{-1} in the control group compared with 61.02 ± 15.14 ng ml^{-1} in the LPAL group ($P<0.05$ *vs.* control group) and 28.43 ± 2.21 ng ml^{-1} in the sham group ($P<0.05$ *vs.* control group). Furthermore, at 5 weeks, the plasma D-dimer concentration remained at high levels (40.28 ± 2.47 ng ml^{-1}) in the LPAL group compared with that of the control (9.37 ± 2.63 ng ml^{-1}; $P<0.05$ *vs.* control) and the sham groups (17.61 ± 2.43 ng ml^{-1}; $P<0.05$ *vs.* sham). At 5 weeks, there was no significant difference between the control and the sham groups. These results revealed that, after LPAL surgery, the rats' plasma D-dimer concentration had increased, and continuous ligation led to a sustained effect to maintain an elevated D-dimer level.

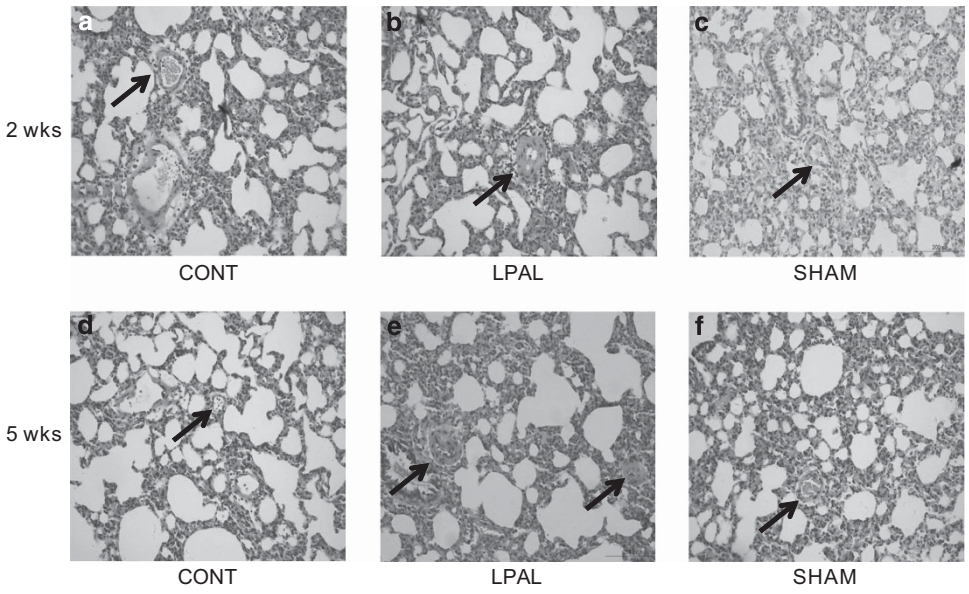

Figure 2 Effects of chronic LPAL on pulmonary vascular remodeling in rats (×200). Lung tissues from CONT, LPAL or SHAM rats at 2 and 5 weeks postsurgery were fixed in 4% paraformaldehyde, embedded in paraffin, cross sectioned (5 μM in thickness) and stained with hematoxylin and eosin. The provided pictures are representative from one of four rats for each group, and the arrows indicate PA in each picture. Pictures (**b**) and (**e**) show the pulmonary arterial wall thickening induced by LPAL, compared with the control (**a**, **d**) and sham surgical groups (**c**, **f**). A full color version of this figure is available at the *Hypertension Research* journal online.

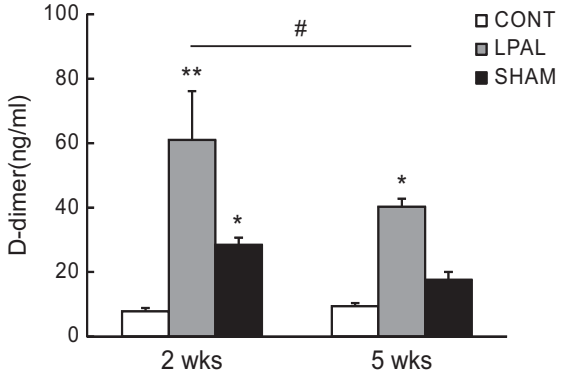

Figure 3 Effects of chronic LPAL on blood plasma D-dimer values (mean ± s.e.m., $n=5$). The bar graph shows the blood plasma D-dimer levels from the CONT, LPAL and SHAM groups. *Indicates a significant difference compared with the respective CONT groups, $P<0.05$; **$P<0.01$ *vs.* CONT group; and $^{\#}P<0.05$ between the 2 and 5 weeks LPAL groups.

LPAL increased the basal $[Ca^{2+}]_i$ and SOCE in freshly isolated rat distal PASMCs

As shown in Figure 4a, at the 2-week time point, the basal $[Ca^{2+}]_i$ in the control group was 104.27 ± 5.38 nM, that in the sham group was 92.98 ± 8.95 nM and that in the LPAL group was 115.83 ± 4.7 nM. The basal $[Ca^{2+}]_i$ showed a slight increase in the LPAL group shortly after the surgery. At the 5-week time point, the difference between the LPAL and the sham groups became more obvious. The basal $[Ca^{2+}]_i$ in the LPAL group was 144.82 ± 5.11 nM, which was significantly higher than that of the sham group (117.62 ± 4.75 nM) ($P<0.01$) and that of the control group (113.86 ± 4.95 nM). Calcium increase during perfusion from calcium-free Krebs to regular Krebs was used to calculate the SOCE peak, as we previously described. Results shown in Figures 4b and c demonstrate that the LPAL groups had significantly higher SOCE peaks ($P<0.01$) than the sham groups at both 2 and 5 weeks. However, there was no difference between the sham and control groups.

LPAL upregulated TRPC1 and TRPC6 mRNA and protein expression in rat distal PA

As shown in Figures 5a and b, LPAL significantly induced increases of TRPC1 and TRPC6 mRNA expression in the rat distal PA. The increases appeared to be significant after 2 weeks of surgery compared with the sham group, while their expression levels went even higher at 5 weeks than the 2-week time point. Figures 5c and d show the TRPC1 and TRPC6 protein expression levels as measured by western blotting. Similarly, compared with the sham groups, LPAL also significantly increased TRPC1 and TRPC6 protein expression levels in the rat distal PA at both 2 and 5 weeks ($P<0.01$). There were no significant differences between the sham and control groups with regards to mRNA and protein levels for either TRPC1 or TRPC6.

DISCUSSION

In this study, we successfully established a stable and reproducible rat model to mimic the pathogenesis of CTEPH, which resembles the human disease. By employing this model, we found that chronically obstructed LPAL led to significant RVH and distal pulmonary arterial remodeling. Our data showed that, after LPAL, at the time points of 2 and 5 weeks postsurgery, plasma D-dimer concentrations were markedly elevated, whereas the sham group rats had a sharp increase after surgery at 2 weeks that then decreased to basal level at 5 weeks. In freshly isolated rat distal PASMCs from rats that received different treatments, we showed that LPAL for 5 weeks resulted in a significant increase of both the basal $[Ca^{2+}]_i$ and SOCE in PASMCs. Furthermore, we found that the expression levels of TRPC1 and TRPC6 were also upregulated. These data indicated that elevation of $[Ca^{2+}]_i$ after LPAL is at least partly due to increased SOCE and the elevated expression of related channel components, suggesting that the

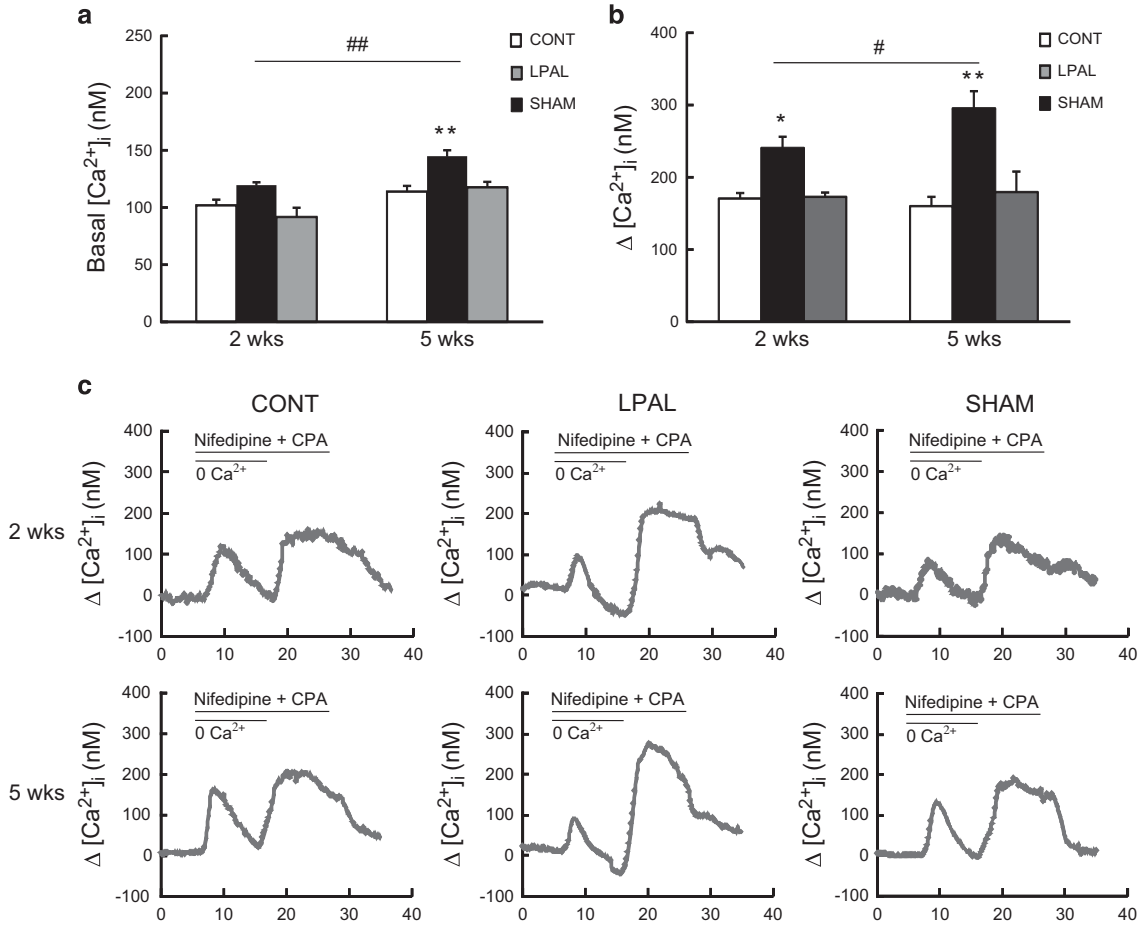

Figure 4 Effects of chronic LPAL on basal $[Ca^{2+}]_i$ and SOCE in rat PASMCs. (**a**) Shows the changes of basal $[Ca^{2+}]_i$ in PASMCs isolated from the CONT, LPAL and SHAM groups. (**b**) Shows the changes of SOCE in PASMCs. (**c**) Represents the trace graphs of SOCE in each group at either 2 or 5 weeks. The SOCE measurements show the delta changes from baseline to the peak of calcium levels. *Indicates a significant difference *vs.* SHAM group, $P<0.05$; **$P<0.01$ *vs.* respective SHAM groups; and $^{\#\#}P<0.01$ between 2 and 5 weeks LPAL groups.

triggered TRPC–SOCE–$[Ca^{2+}]$i signaling axis has a crucial role in the pathogenesis of LPAL-induced CTEPH.

Previous animal models of postembolic PH mostly involved large animals (pigs and dogs).[4,18] Several animal models have been developed to study the pathophysiology of CTEPH, in which acute pulmonary embolism is easily produced; however, the instability of the embolism makes it difficult to design a study based only on PA. Therefore, their studies were based on whole lung tissue and focused on the thrombus resolution, inflammation and angiogenesis of the pulmonary embolism.[19] Our LPAL model allowed us to develop a stable obstruction from one lobe of the PA and use the PA in unobstructed territories to study the mechanism of pulmonary arterial remodeling in CTEPH. Jungebluth *et al.*[3] reported increased mean PA pressure and PVR, RVH, low cardiac output and capillaritis in the right lung (as an indication of inflammation), as well as the muscularization of the PA after 2 weeks of LPAL surgery. Consistent with previous reports, our results in this study indicated that LPAL can induce rat distal PA wall thickness, increase RVSP and eventually lead to RVH at 5 weeks after LPAL surgery. In addition, we also detected significantly elevated plasma D-dimer levels. D-dimer is a fibrin degradation product and is a small protein fragment present in the blood after a blood clot is degraded by fibrinolysis.[20,21] Since its discovery in the 1990s, it has become an important part of blood tests performed on patients suspected of having thrombotic disorders, such as deep venous thrombosis, pulmonary embolism and disseminated intravascular coagulation. The results showed a sharp increase of D-dimer values 2 weeks after LPAL in both the surgical groups (LPAL and sham groups). However, the plasma D-dimer level maintained a high level after 5 weeks in the LPAL group, while it went down in the sham group. This finding indicates that the animals from the LPAL group continuously maintained a pro-coagulant state after the surgery. Another advantage of our animal models is that, after chronic ligation in the PA of left lobe, the left lung shows visual atrophy after ligation and increased right lobe volume compared with that of the sham group, likely indicating a compensation mechanism after the left lobe's obstruction. Elizabeth's study showed that the normal right lung lobe had increased flow and shear stress, in addition to the obstruction of the large PA, but total lung volume was not altered.[5] Similarly, in clinics, patients have also been shown to develop vascular lesions in distal unobstructed territories.[22] These findings suggest that chronic LPAL-induced CTEPH in rats represents morphological and functional similarity to those clinical PH patients who are diagnosed with this type of PH.

A number of mechanisms that cause PH have been explored to explain how CTEPH patients developed persistent PH, for instance, the crucial role of endothelial cell damage.[6,7,12] In this study, we mostly focused on the role of PASMCs, which comprise the muscular bulk of the vascular wall. CTEPH patients demonstrate extensive

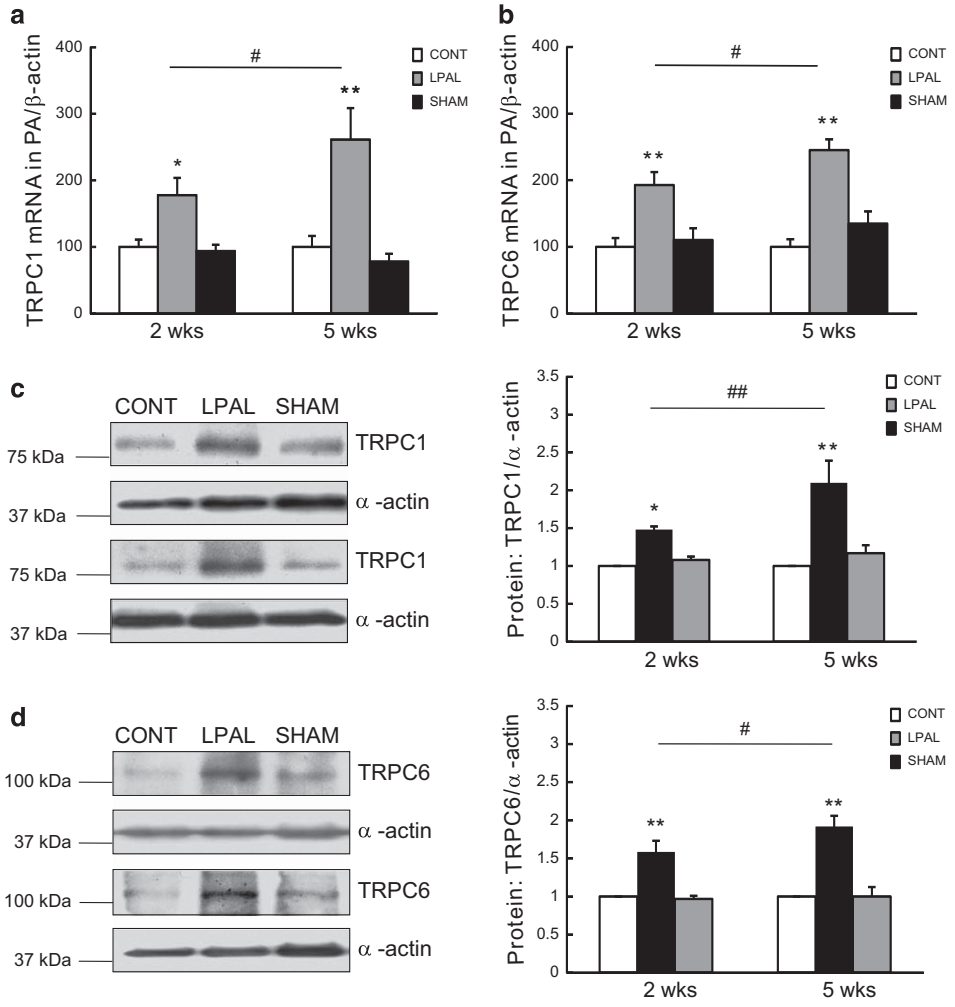

Figure 5 Effects of chronic LPAL on TRPC1 and TRPC6 mRNA and protein expression in rat distal pulmonary artery smooth muscle (mean ± s.e.m., $n=5$). TRPC1 (**a**) and TRPC6 (**b**) mRNA relative to β-actin was detected by real-time quantitative PCR. Expression of TRPC1 and TRPC6 proteins levels were measured by western blotting (**c** and **d**). Representative blots (**c** and **d**) and mean intensity for TRPC1 or TRPC6 blots relative to α-actin. *Indicates a significant difference *vs.* SHAM group, $P<0.05$; **$P<0.01$ *vs.* respective SHAM groups; $^{\#}P<0.05$ between 2 and 5 weeks LPAL groups; and $^{\#\#}P<0.01$ between the 2 and 5weeks LPAL groups.

medial PA wall thickening presumably owing to increased PASMC proliferation. As we know, cytosolic free Ca^{2+} concentration and SOCE are known to be important factors in mediating PASMC proliferation and vascular remodeling in PH.[8,9,23] SOCE is one of the three main mechanisms to mediate extracellular calcium influx. The other two are voltage-dependent calcium channel-mediated calcium influx, the regulation of which is controlled by changes in membrane potential, and receptor-operated calcium channel-mediated calcium influx, which is initiated by specific binding between the membrane receptor and the corresponding ligand.[15] As we know, SOCE is initiated and activated by sarcoplasmic reticulum calcium store depletion. Previously, we and others have confirmed that in chronic hypoxia-induced pulmonary hypertension rats, chronic hypoxia contributes to increased $[Ca^{2+}]_i$, which is mostly caused by enhanced SOCE through SOCC.[13] Moreover, Ogawa *et al.*[24] found that the Akt/mTOR (mammalian target of rapamycin) pathway is involved in growth factor-mediated SOCE in human PASMCs and mediates pulmonary vascular remodeling in CTEPH, suggesting a potential therapeutic benefit for the inhibition of mTOR (for example, via the mTOR inhibitor rapamycin) in these patients. Their study actually confirmed our results that basal $[Ca^{2+}]_i$ and SOCE, measured via Ca^{2+} restoration following store depletion, were greater in PASMCs from LPAL rats compared with the PASMCs from sham and control rats. Their data suggest that chronic LPAL could enhance SOCE and elevate basal $[Ca^{2+}]_i$ in PASMCs.

One possible cause of enhanced SOCE following LPAL is the increased expression of SOCC components. The TRPC subunits TRPV and TRPM may also participate. TRPV4 operates as a mechanosensitive cation channel in PASMCs, is stimulated by abnormal osmolarity, pressure and heat and shear stress and is upregulated in PA in chronic hypoxia-induced PH rats.[25,26] TRPM8, also known as the cold and menthol receptor 1, is downregulated in both hypoxia-induced and monocrotaline-induced PH models and is associated with menthol-induced vasorelaxation.[24] Of all the TRPCs, TRPC1, TRPC4 and TRPC6 are predominantly expressed in the distal PA and PASMCs.[15] Furthermore, our previous studies found that, in rat models, chronic hypoxia could induce the expression of TRPC1 and TRPC6 but not TRPC4. Considering the increased TRPC expression, the intracellular calcium homeostasis and the development of CTEPH, it is reasonable to hypothesize that LPAL-induced PH is

potentially mediated via the regulation of the TRPC–SOCE–$[Ca^{2+}]_i$ signaling cascade. Direct evidence from our data indicate that the effective small interfering RNA knockdown of TRPC1 or TRPC6 expression significantly reduced the hypoxia-increased SOCE and basal $[Ca^{2+}]_i$ in PASMCs. In addition to our data, recent data from other groups' studies using transgenic knockout mice strategies have also shown strong evidence to support the relationship between the reported molecular mechanisms (such as TRPC-SOCE) and physiological parameters (such as pulmonary vascular tone and pressure). In detail, by using transgenic TRPC1 knockout mice, a study from Dr Weissmann's laboratory revealed that, during the progression of CHPH, the hypoxia-induced pulmonary vascular remodeling is, at least partly, driven by TRPC1. Almost at the same time in another parallel study using both TRPC1 and TRPC6 knockout mice, Xia *et al.* also provided direct evidence showing that TRPC1 and TRPC6 are crucial for the regulation of hypoxia-triggered vasoreactivity and other systemic hemodynamic parameters, such as RVSP, RVH and histological thickening.[27–29] As mentioned above, chronic LPAL in rats induced elevated $[Ca^{2+}]_i$ and SOCE in PASMCs. LPAL could significantly induce TRPC1 and TRPC6 expression at both the mRNA and protein level in the distal PA. Furthermore, TRPC1 and TRPC6 mRNA and protein expression were even higher at 5 weeks after LPAL surgery compared with that at 2 weeks. These results suggest that upregulation of TRPC1 and TRPC6 expression might act as a key driver behind the increased basal $[Ca^{2+}]_i$ and SOCE activity elevation in PASMCs from the LPAL-induced CTEPH animal model.

According to several recent clinical trials, some drugs such as prostanoids, endothelin receptor antagonists and phosphodiesterase type-5 inhibitors did provide encouraging treatment results for PH patients.[30,31] Therefore, medical therapy may also potentially benefit the CTEPH patients deemed non-operable and those with persistent PH following pulmonary endarterectomy. Recently, some publications have shown that an old class of clinical medication might have new effects on PH by targeting TRPC. These medications include digoxin (used to treat heart failure on the basis of its inotropic potential),[32] tanshinone IIA sulfonate (a water-soluble derivative isolated from a widely used traditional Chinese medicine commonly administered to treat inflammatory and cardiovascular diseases)[33] and sildenafil. Particularly sildenafil, a potent and selective type V phosphodiesterase inhibitor, has recently been well studied in a couple of clinical trials of CTEPH. These studies have shown that patients treated with sildenafil have a significant decrease in mean pulmonary artery pressure, increased peak exercise right ventricular ejection fraction and improvements in exercise capacity.[34–36] However, the detailed mechanisms are not yet fully understood. Our group's previous study with sildenafil demonstrated that the drug attenuates PH in association with reduced SOCE and normalized TRPC1 and TRPC6 expression in rat distal PASMCs via a cGMP–protein kinase G–peroxisome proliferator-activated receptor (PPAR) gamma-dependent mechanism.[16] Yang *et al.*[37] found that PPAR gamma activation can impair the disrupted classic bone morphogenetic proteins/Smad/ID1 signaling axis, which was shown to be protective to PASMC proliferation and PA remodeling during PH disease development. In this study, we confirmed that the LPAL model of CTEPH also exhibits elevated SOCE and upregulated TRPC1 and TRPC6 expression in PA, suggesting the CTEPH might share similar mechanisms during disease development and might benefit from similar treatment strategies as other types of PH models.

In summary, in this study we generated a stable rat model by using surgical LPAL to mimic CTEPH and found for the first time that in PASMCs (1) chronic LPAL can significantly upregulate TRPC1 and TRPC6 expression at both the mRNA and protein level and (2) the LPAL-increased SOCE and basal $[Ca^{2+}]_i$, owing to the upregulation of the TRPC proteins, might account at least partly for CTEPH pathogenesis and might be potential targets for future treatment of CTEPH.

CONFLICT OF INTEREST

The authors declare no conflict of interest.

ACKNOWLEDGEMENTS

This work was supported by an NIH Research Grant (R01HL093020), the National Natural Science Foundation of China (81173112, 81170052, 81220108001), a Guangdong Natural Science Foundation team grant (2010) and a Guangzhou Department of Education Yangcheng Scholarship (12A001S).

1 Galie N, Hoeper MM, Humbert M, Torbicki A, Vachiery JL, Barbera JA, Beghetti M, Corris P, Gaine S, Gibbs JS, Gomez-Sanchez MA, Jondeau G, Klepetko W, Opitz C, Peacock A, Rubin L, Zellweger M, Simonneau G, ESC Committee for Practice Guidelines (CPG). Guidelines for the diagnosis and treatment of pulmonary hypertension. *Eur Respir J* 2009; **34**: 1219–1263.
2 Lang IM, Madani M. Update on chronic thromboembolic pulmonary hypertension. *Circulation* 2014; **130**: 508–518.
3 Jungebluth P, Ostertag H, Macchiarini P. An experimental animal model of post-obstructive pulmonary hypertension. *J Surg Res* 2008; **147**: 75–78.
4 Mercier O, Fadel E. Chronic thromboembolic pulmonary hypertension: animal models. *Eur Respir J* 2013; **41**: 1200–1206.
5 Wagner EM, Jenkins J, Perino MG, Sukkar A, Mitzner W. Lung and vascular function during chronic severe pulmonary ischemia. *J Appl Physiol (1985)* 2011; **110**: 538–544.
6 Nijkeuter M, Hovens MM, Davidson BL, Huisman MV. Resolution of thromboemboli in patients with acute pulmonary embolism: a systematic review. *Chest* 2006; **129**: 192–197.
7 Sacks RS, Remillard CV, Agange N, Auger WR, Thistlethwaite PA, Yuan JX. Molecular biology of chronic thromboembolic pulmonary hypertension. *Semin Thorac Cardiovasc Surg* 2006; **18**: 265–276.
8 Shimoda LA, Laurie SS. Vascular remodeling in pulmonary hypertension. *J Mol Med (Berl)* 2013; **91**: 297–309.
9 Shimoda LA, Semenza GL. HIF and the lung: role of hypoxia-inducible factors in pulmonary development and disease. *Am J Respir Crit Care Med* 2011; **183**: 152–156.
10 Rabinovitch M. Molecular pathogenesis of pulmonary arterial hypertension. *J Clin Invest* 2008; **118**: 2372–2379.
11 Guo Q, Huang JA, Yamamura A, Yamamura H, Zimnicka AM, Fernandez R, Yuan JX. Inhibition of the Ca(2+)-sensing receptor rescues pulmonary hypertension in rats and mice. *Hypertens Res* 2014; **37**: 116–124.
12 Zabini D, Nagaraj C, Stacher E, Lang IM, Nierlich P, Klepetko W, Heinemann A, Olschewski H, Bálint Z, Olschewski A. Angiostatic factors in the pulmonary endarterectomy material from chronic thromboembolic pulmonary hypertension patients cause endothelial dysfunction. *PLoS One* 2012; **7**: e43793.
13 Wang J, Weigand L, Lu W, Sylvester JT, Semenza GL, Shimoda LA. Hypoxia inducible factor 1 mediates hypoxia-induced TRPC expression and elevated intracellular Ca2+ in pulmonary arterial smooth muscle cells. *Circ Res* 2006; **98**: 1528–1537.
14 Ogawa A, Firth AL, Ariyasu S, Yamadori I, Matsubara H, Song S, DR Fraidenburg, Yuan JX. Thrombin-mediated activation of Akt signaling contributes to pulmonary vascular remodeling in pulmonary hypertension. *Physiol Rep* 2013; **1**: e00190.
15 Wang J, Shimoda LA, Sylvester JT. Capacitative calcium entry and TRPC channel proteins are expressed in rat distal pulmonary arterial smooth muscle. *Am J Physiol Lung Cell Mol Physiol* 2004; **286**: L848–L858.
16 Wang J, Yang K, Xu L, Zhang Y, Lai N, Jiang H, Zhang Y, Zhong N, Ran P, Lu W. Sildenafil inhibits hypoxia induced TRPC expression in pulmonary arterial smooth muscle via cGMP-PKG-PPARgamma axis. *Am J Respir Cell Mol Biol* 2013; **49**: 231–240.
17 Wang J, Xu L, Yun X, Yang K, Liao D, Tian L, Jiang H, Lu W. Proteomic analysis reveals that proteasome subunit beta 6 is involved in hypoxia-induced pulmonary vascular remodeling in rats. *PLoS One* 2013; **8**: e67942.
18 Sage E, Mercier O, Van den Eyden F, de Perrot M, Barlier-Mur AM, Dartevelle P, Eddahibi S, Herve P, Fadel E. Endothelial cell apoptosis in chronically obstructed and reperfused pulmonary artery. *Respir Res* 2008; **9**: 19.
19 Zagorski J, Debelak J, Gellar M, Watts JA, Kline JA. Chemokines accumulate in the lungs of rats with severe pulmonary embolism induced by polystyrene microspheres. *J Immunol* 2003; **171**: 5529–5536.
20 Runyon MS, Gellar MA, Sanapareddy N, Kline JA, Watts JA. Development and comparison of a minimally-invasive model of autologous clot pulmonary embolism in Sprague-Dawley and Copenhagen rats. *Thromb J* 2010; **8**: 3.

21 Watts JA, Lee YY, Gellar MA, Fulkerson MB, Hwang SI, Kline JA. Proteomics of microparticles after experimental pulmonary embolism. *Thromb Res* 2012; **130**: 122–128.
22 Hoeper MM, Mayer E, Simonneau G, Rubin LJ. Chronic thromboembolic pulmonary hypertension. *Circulation* 2006; **113**: 2011–2020.
23 Golovina VA. Cell proliferation is associated with enhanced capacitative Ca(2+) entry in human arterial myocytes. *Am J Physiol* 1999; **277**: C343–C349.
24 Ogawa A, Firth AL, Yao W, Madani MM, Kerr KM, Auger WR, Jamieson SW, Thistlethwaite PA, Yuan JX. Inhibition of mTOR attenuates store-operated Ca2+ entry in cells from endarterectomized tissues of patients with chronic thromboembolic pulmonary hypertension. *Am J Physiol Lung Cell Mol Physiol* 2009; **297**: L666–L676.
25 Song S, Yamamura A, Yamamura H, Ayon RJ, Smith KA, Tang H, Makino A, Yuan JX. Flow shear stress enhances intracellular Ca2+ signaling in pulmonary artery smooth muscle cells from patients with pulmonary arterial hypertension. *Am J Physiol Cell Physiol* 2014; **307**: C373–C383.
26 Liu XR, Liu Q, Chen GY, Hu Y, Sham JS, Lin MJ. Down-regulation of TRPM8 in pulmonary arteries of pulmonary hypertensive rats. *Cell Physiol Biochem* 2013; **31**: 892–904.
27 Lu W, Ran P, Zhang D, Peng G, Li B, Zhong N, Wang J. Sildenafil inhibits chronically hypoxic upregulation of canonical transient receptor potential expression in rat pulmonary arterial smooth muscle. *Am J Physiol Cell Physiol* 2010; **298**: C114–C123.
28 Malczyk M, Veith C, Fuchs B, Hofmann K, Storch U, Schermuly RT, Witzenrath M, Ahlbrecht K, Fecher-Trost C, Flockerzi V, Ghofrani HA, Grimminger F, Seeger W, Gudermann T, Dietrich A, Weissmann N. Classical transient receptor potential channel 1 in hypoxia-induced pulmonary hypertension. *Am J Respir Crit Care Med* 2013; **188**: 1451–1459.
29 Xia Y, Yang XR, Fu Z, Paudel O, Abramowitz J, Birnbaumer L, Sham JS. Classical transient receptor potential 1 and 6 contribute to hypoxic pulmonary hypertension through differential regulation of pulmonary vascular functions. *Hypertension* 2014; **63**: 173–180.
30 Nishimura R, Tanabe N, Sugiura T, Shigeta A, Jujo T, Sekine A, Sakao S, Kasahara Y, Tatsumi K. Improved survival in medically treated chronic thromboembolic pulmonary hypertension. *Circ J* 2013; **77**: 2110–2117.
31 Pepke-Zaba J, Jansa P, Kim NH, Naeije R, Simonneau G. Chronic thromboembolic pulmonary hypertension: role of medical therapy. *Eur Respir J* 2013; **41**: 985–990.
32 Abud EM, Maylor J, Undem C, Punjabi A, Zaiman AL, Myers AC, Sylvester JT, Semenza GL, Shimoda LA. Digoxin inhibits development of hypoxic pulmonary hypertension in mice. *Proc Natl Acad Sci USA* 2012; **109**: 1239–1244.
33 Wang J, Jiang Q, Wan L, Yang K, Zhang Y, Chen Y, Wang E, Lai N, Zhao L, Jiang H, Sun Y, Zhong N, Ran P, Lu W. Sodium tanshinone IIA sulfonate inhibits canonical transient receptor potential expression in pulmonary arterial smooth muscle from pulmonary hypertensive rats. *Am J Respir Cell Mol Biol* 2013; **48**: 125–134.
34 Wei L, Zhu W, Xia L, Yang Y, Liu H, Shen J, Zhu J, Xu Y, Yang Z, Wang C. Therapeutic effect of eNOS-transfected endothelial progenitor cells on hemodynamic pulmonary arterial hypertension. *Hypertens Res* 2013; **36**: 414–421.
35 Zhuang Y, Jiang B, Gao H, Zhao W. Randomized study of adding tadalafil to existing ambrisentan in pulmonary arterial hypertension. *Hypertens Res* 2014; **37**: 507–512.
36 Claessen G, La Gerche A, Wielandts JY, Bogaert J, Van Cleemput J, Wuyts W, Claus P, Delcroix M, Heidbuchel H. Exercise pathophysiology and sildenafil effects in chronic thromboembolic pulmonary hypertension. *Heart* 2015; **101**: 637–644.
37 Yang J, Li X, Al-Lamki RS, Wu C, Weiss A, Berk J, Schermuly RT, Morrell NW. Sildenafil potentiates bone morphogenetic protein signaling in pulmonary arterial smooth muscle cells and in experimental pulmonary hypertension. *Arterioscler Thromb Vasc Biol* 2013; **33**: 34–42.